Comparison of the DC/DC-Converters for Fuel Cell Applications

Oleksandr Krykunov

Abstract—The source voltage of high-power fuel cell shows strong load dependence at comparatively low voltage levels. In order to provide the voltage of 750V on the DC-link for feeding electrical energy into the mains via a three phase inverter a step-up converter with a large step-up ratio is required. The output voltage of this DC/DC-converter must be stabile during variations of the load current and the voltage of the fuel cell. This paper presents the methods and results of the calculation of the efficiency and the expense for the realization for the circuits of the DC/DC-converter that meet these requirements.

Keywords—DC/DC-converter, calculation, efficiency, fuel cell.

I. INTRODUCTION

THIS paper presents the methods and results of the comparison of circuits of the DC/DC-converter for the output power of 5 kW and the output voltage of 750V. In the Section II the used structures of the 5kW-fuel cell systems are shown. Section III provides the mathematical analysis of the chosen circuits of the DC/DC-converter, design of these circuits. In Section IV the methods and results of comparison of the DC/DC-converters are presented.

II. STRUCTURES OF THE ELECTRICAL FUEL CELL SYSTEM

In [1] the typical structures of the electrical fuel cell system are presented. For the reasons of the controllability, reliability and the low cost the structure, which is shown in Fig.1 is chosen. The DC/DC-converter with galvanic isolation provides the isolation of the fuel cell potential from the grid.
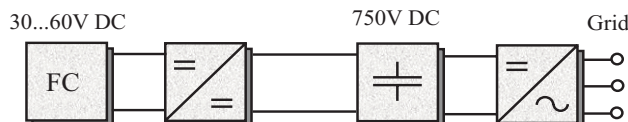

Fig. 1 The structure of the electrical fuel cell system for the DC/DC-converter with galvanic isolation.

In the case of the DC/DC-converter without galvanic isolation the structure, that is shown in Fig. 2, should be used. The configuration shown in the Fig. 2 is in [2] described. The power that flows through each DC/DC-converter is a half of the input power. For DC/DC-converter without galvanic isolation, the losses in the one of the DC/DC-converters must be calculated for the output power of 2.5kW and must be doubled.
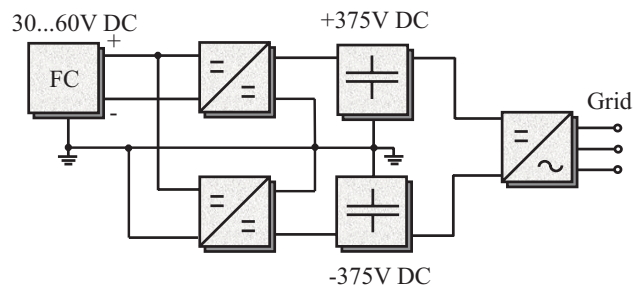
Fig. 2 The structure of the electrical fuel cell system for the DC/DC-converter without galvanic isolation.

The result is a total loss for two DC/DC-converters.

III. MATHEMATICAL ANALYSIS OF THE CIRCUITS OF DC/DC-CONVERTERS FOR THE FUEL CELL SYSTEM

A. Choice of the investigated circuits

The DC/DC-converter for fuel cell applications must be fit into the requirements:

- high step-up conversion ratio
- high stability of the output voltage during the variations of the output current and the input voltage
- high efficiency
- low cost

The first requirement excludes all circuits without a transformer. High step-up conversion ratio is in these circuits provided only at extreme high duty cycles, which are not acceptable [3]. The second requirement excludes all circuits for which a controller cannot be designed for a stable output voltage [4]. A transferred power of 5kW is another key value for choosing the circuits for the investigation. In some circuits the design of the transformer for this power results in a large size of the transformer, another circuits have problems with the saturation of the transformer [5]. These circuits will not be investigated. The following factors can result in high efficiency and low cost of the converter [6]:

- low current or voltage stresses of the semiconductors
- utilization of the of the B-H-characteristic of the transformer in all quadrants
- low input current ripple
- low number of components
- simple design of the transformer

All the circuits, that combine some of these benefits, will be investigated and are shown in the Fig.3. The circuits were investigated for the ideal transformer. The leakage inductances of the transformer were not considered.
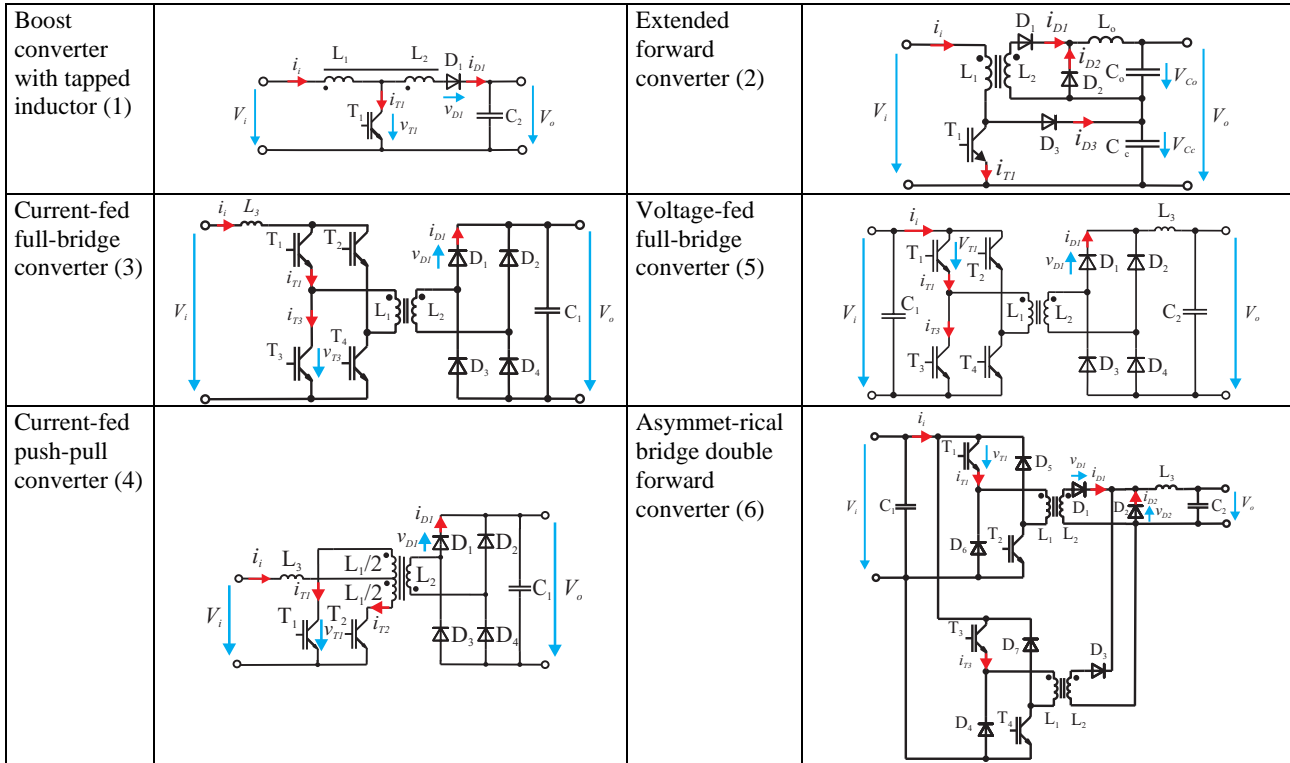
Fig. 3 Investigated step-up DC/DC-converter circuits

The parameter of each circuit (turns ratio of the transformer, duty cycle) has a great influence on the efficiency of each circuit. The following values change with the variation of the duty cycle:

- rms and average values of the switch and diode currents
- blocking voltage of the switches and diodes
- size of the transformer

Hence the optimal duty cycle for each circuit exists, at which the efficiency of the circuit is maximum. For this duty cycle the above-named values must be calculated. For some circuits the estimation of this duty cycle is quite complex. This paper provides some criteria for the choosing of the optimal duty cycle. With the help of these criteria the duty cycle for each circuit will be determined.

A. Boost converter wit tapped inductor

The boost converter with tapped inductor provides no galvanic isolation an hence should be connected to the fuel cell as shown in the Fig. 2. Each of the boost converter must provide a maximum step-up ratio of 12,5 for variation of the input voltage $V_i = 30\ldots60V$. The maximum input current occurs at the minimum input voltage and hence the efficiency of the converter is minimum at the minimum input voltage. This efficiency will be calculated. The maximum duty cycle is determined as (Fig.4):

$$D = \frac{t_1 - t_o}{T} \qquad (1)$$

With T- switching period, and for the turns ratio of the tapped inductor $\ddot{u} = W_2 / W_1 = 4$ can be calculated [6]:

$$D = \frac{V_o / V_i - 1}{V_o / V_i + W_2 / W_1} = \frac{12,5 - 1}{12,5 + 4} \approx 0,73 \qquad (2)$$

It was shown in [7] that the losses in the clamping-circuit are at this duty cycle minimum. The simulated waveforms of the boost converter with tapped inductor for these parameters are shown in the Fig. 4. The rms values of the switch current, diode current and the input current can be calculated regarding to the functions $i_{T1}(t), i_{D1}(t)$ in [6]:

$$I_{T1,RMS} = \frac{\sqrt{3}}{3} \sqrt{\frac{V_i^2 D^3 T^2}{L_1^2} + \frac{3V_i D^2 T I_{1,min}}{L_1} + 3D I_{1,min}^2} \qquad (3)$$

$$I_{D1,RMS} = \sqrt{\frac{1}{T}\left(\frac{1}{3}\frac{I_{2,max}^2 L_1(1+\ddot{u})^2}{V_o - V_i} - \frac{\left(L_1 I_{2,max}(1+\ddot{u})^2 + (1-D)T(V_i - V_o)\right)^3}{3L_1^2(V_o - V_i)(1+\ddot{u})^2}\right)} \qquad (4)$$

$$I_{i,RMS} = \sqrt{\frac{1}{T}\left(\frac{1}{3}\frac{I_{2,max}^2 L_1(1+\ddot{u})^2}{V_o - V_i} - \frac{\left(L_1 I_{2,max}(1+\ddot{u})^2 + (1-D)T(V_i - V_o)\right)^3}{3L_1^2(V_o - V_i)(1+\ddot{u})^2} + B_1\right)} \qquad (5)$$

with

$$B_1 = \frac{DT}{3L_1^2}(V_i^2 D^2 T^2 + 3V_i DT I_{1,min} L_1 + 3I_{1,min}^2 L_1^2)$$

$I_{1,min} = i_{T1}(t_0)$ - minimum switch current,

$I_{2,\max} = i_{D1}(t_1)$ - maximum diode current.

The average value of the input current and the diode current can be calculated regarding to the functions $i_{T1}(t), i_{D1}(t)$ in [6]:
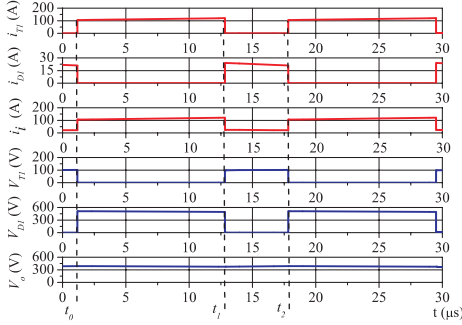

Fig. 4 Simulated waveforms of the boost converter with tapped inductor

$$I_{D1,avg} = 0.5(1-D)^2 TL_1^{-1}\left(V_i - V_o(1+\ddot{u})^{-2}\right) + (1-D)I_{2,\max} \quad (6)$$

$$I_{i,avg} = 0{,}5TL_1^{-1}B_2 + (1-D)I_{2,\max} + I_{1,\min}D \quad (7)$$

With $B_2 = V_i(1-D)^2 - V_o(1-D)^2(1+\ddot{u})^{-2} + V_iD^2 \quad (8)$

The blocking voltages of the switch and the diode were calculated in [6] as follows:

$$V_{T1} = (V_o - V_i)/(W_1 + W_2) + V_i \quad (9)$$

$$V_{D1} = (V_o - V_i)/(W_1 + W_2)(W_2/W_1 - 1) + V_o - V_i \quad (10)$$

It can be seen from the Fig. 4 that the switch and the diode are turned on and turned off at their full blocking voltage. At the time t_2 the diode D_1 is switched off and the switch T_1 is switched on. The current of the diode D_1 falls to zero and the current of the switch T_1 rises. This commutation phase occurs in consideration of the leakage inductances of the tapped inductor and results in the hard turn on of the switch T_1. The reverse-recovery current of the diode D_1 at turn off results in the over current at the switching on of the switch T_1. This over current can be calculated:

$$\Delta i_{T1,on} = I_{RM,D1}(1 + W_2/W_1) \quad (11)$$

B. Extended forward converter

The extended forward converter was proposed and mathematically analysed in [2]. This converter provides no galvanic isolation an hence should be connected to the fuel cell as shown in the Fig. 2. Each of the boost converter must provide a maximum step-up ratio of 12,5 for variation of the input voltage $V_i = 30\ldots60V$. It was shown in [2] that the output voltage in steady-state if the voltage ripple of the capacitors is low can be calculated as follows:

$$V_o = V_{Co} + V_{Cc} = V_i \ddot{u} D + \frac{V_i}{1-D} \quad (12)$$

The blocking voltages of the diodes D_1, D_2, D_3 and the blocking voltage of the switch can be calculated as in [7]:

$$V_{D1} = \left(\frac{V_i}{1-D} - V_i\right)\ddot{u} \quad (13)$$

$$V_{D2} = V_i \ddot{u} \quad (14)$$

The voltage V_{Cc} is the blocking voltage of the switch. It can be seen from (12) that this voltage strong increases with the increase of the duty cycle. To minimize the blocking voltage of the switch the possibly minimum duty cycle must be chosen. From (13), (14) it can be shown that the design of the circuit for the duty cycles lower than 55% results in the use of high-blocking voltage diodes (>1,2 kV).For these reasons the turns ratio of the transformer $\ddot{u} = 18$ at the maximum duty cycle of 0,57 at the input voltage of 30V was determined. The simulated waveforms of the extended forward converter for these parameters are shown in the Fig. 5.
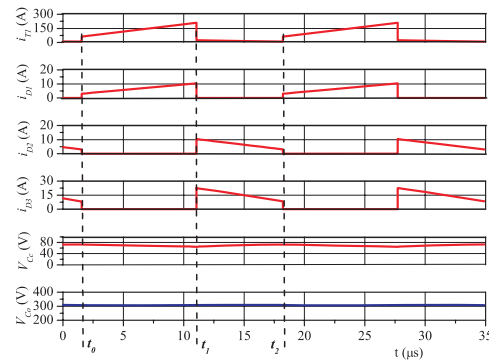

Fig. 5 Simulated waveforms of the extended forward converter

The average and rms values of the diode currents, switch current and the input current can be calculated:

$$I_{D1,avg} = I_{2,\min}D + \left(V_i - V_i\ddot{u}D\right)D^2 TL_o^{-1} \quad (15)$$

$$I_{D2,avg} = \frac{T(D^2-1)V_i\ddot{u}D + 2V_i\ddot{u}DT(1-D)}{2L_o} + I_{2,\min}(1-D) \quad (16)$$

$$I_{D3,avg} = (1-D)\left(I_{1,\min} - I_{2,\min}\ddot{u}\right) + \frac{V_i\left(1-D^2\right)T - V_i(1-D)T}{2L_1} \quad (17)$$

$$I_{i,avg} = I_{1,\min} - I_{2,\min}\ddot{u}(1-D) + DT\frac{V_i}{L_1} + D^2 TV_i\ddot{u}^2\frac{1-D}{L_o} \quad (18)$$

$$I_{T1,RMS} = \sqrt{\frac{1}{T}\left(I_{1,\min}^2 DT + V_iD^2T^2\frac{I_{1,\min}}{L_1} + \frac{1}{3}V_i^2D^3\frac{T^3}{L_1^2}\right) + \frac{\left(V_i\ddot{u}^2 - V_i\ddot{u}^2D\right)\left(D^2T^2I_{1,\min} + \frac{2}{3}\frac{V_i}{L_1}D^3T^3\right)}{L_o} + \frac{1}{3}\frac{\ddot{u}^2D^3T^3}{L_o^2}\left(V_i^2\ddot{u}^2 - 2DV_i^2\ddot{u}^2 + V_i^2\ddot{u}^2D^2\right)} \quad (19)$$

$$I_{D1,RMS} = \sqrt{\frac{1}{TL_o^2}\left(\frac{1}{3}V_i^2\ddot{u}^2D^2D^3T^3 + DT\left(\frac{1}{3}V_i^2D^2T^2\ddot{u}^2 + V_i\ddot{u}DTL_oI_{2,\min} + I_{2,\min}^2L_o^2\right) + V_i\ddot{u}D^3T^2\left(-\frac{2}{3}V_i\ddot{u}DT - I_{2,\min}L_o\right)\right)} \quad (20)$$

$$I_{i,RMS} \sqrt{ \frac{\left(\left(I_{1,min} + V_i DT \frac{L_o + L_1 \ddot{u}^2 - L_1 D \ddot{u}^2}{L_1 L_o} \right)^3 - I_{1,min}{}^3 \right) L_1 L_o}{3 V_i T \left(L_o + L_1 \ddot{u}^2 - L_1 D \ddot{u}^2 \right)} + \frac{\left(\left(I_{1,min} - I_{2,min}\ddot{u} + \frac{V_i}{L_1} DT \right)^3 - \left(I_{1,min} - I_{2,min}\ddot{u} \right)^3 \right) L_1 (1-D)}{3 V_i DT} } \tag{21}$$

$$I_{D3,RMS} = \sqrt{ \frac{\left(\left(I_{1,min} - I_{2,min}\ddot{u} + \frac{V_i}{L_1} DT \right)^3 - \left(I_{1,min} - I_{2,min}\ddot{u} \right)^3 \right) L_1 (1-D)}{3 V_i DT} } \tag{22}$$

$$I_{D2,RMS} = \sqrt{ \frac{\left(I_{2,min} + \frac{V_i \ddot{u} DT - V_i \ddot{u} D^2 T}{L_o} \right)^3 L_o{}^3 - \left(V_i \ddot{u} DT + I_{2,min} L_o - V_i \ddot{u} DT \right)}{3 T L_o{}^2 V_i \ddot{u} D} } \tag{23}$$

With $I_{1,min} = i_1(t_0)$ - minimum switch current,

$I_{2,max} = i_2(t_1)$ - minimum diode current.

The blocking voltage of the switch can be calculated:

$$V_{T1} = V_{Cc} = \frac{V_i}{1-D} \tag{24}$$

The switch and the diode are turned on and turned off at their full blocking voltage. It is important for the calculation of the switching losses of the switch and the diode. The choice of semiconductors for the switch must be done recording to the maximum blocking voltage of the switch:

$$V_{T1,mac} = \frac{V_{i,max}}{1-D} \tag{25}$$

It can be seen from the Fig. 5 that the same commutation phase as for the boost converter with tapped inductor at turn on of the switch T_1 occurs. The over current at turn on of the switch T_1 can be calculated:

$$\Delta i_{T1,on} = I_{RM,D1} \tag{26}$$

C. Current- fed full-bridge converter

The current-fed full-bridge converter was mathematically analysed in [8]. This converter provides a galvanic isolation and hence should be connected to the fuel cell as shown in the Fig. 1. The step-up conversion ratio can be, as shown in [8], calculated:

$$\frac{V_o}{V_i} = \frac{\ddot{u}}{(1 - 2t_{ov}/T)} \tag{27}$$

with $t_{ov} = t_2 - t_1 = t_4 - t_3 = T(D - 0,5)$, $D > 0,5$ (28)

-time period, where all transistors are on, $T = t_4 - t_0$ -switching period.The blocking voltages of the transistor and the secondary diodes can be, as shown in [8], calculated:

$$V_{T1} = V_o / \ddot{u} \tag{29}$$

$$V_{D1} = V_o \tag{30}$$

To reduce the blocking voltage of the transistor the maximum turns ratio of the transformer is needed. The solution of (27) for the turns ratio is:

$$\ddot{u}_{max} = 2V_o(1 - D_{min}) / V_{i,max} = 2 \cdot 750V \cdot (1 - 0,5) / 60V \approx 12 \tag{31}$$

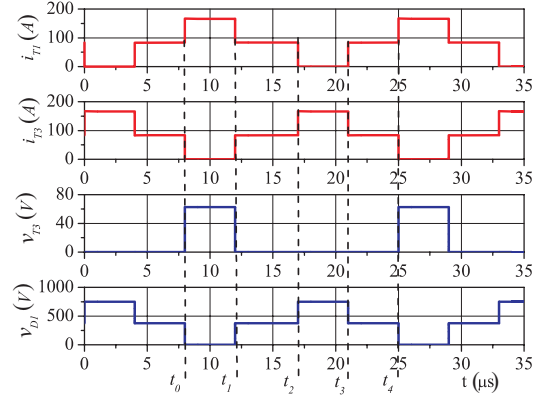The simulation results for these parameters are shown in the Fig. 6.

Fig. 6 Simulated waveforms of the current-fed full-bridge converter

It can be seen from Fig. 6 that the switch T_3 is switched off at the time t_0 at the full blocking voltage. At the time t_1 the switch T_3 is switched on. The current of the switch T_3 rises and the current of the switch T_1 falls until the input current distributes equally between these switches. This commutation phase results in the hard turn on of the switch. At the time t_1 the diode D_1 is switched off. The reverse-recovery current of the diode D_1 results in the over current at the switching on of the switch T_3. This over current can be calculated:

$$\Delta i_{T1,on} = 0,5 I_{RM,D1}\ddot{u} \tag{32}$$

with $I_{RM,D1}$ – reverse-recovery current of the diode D_1

The time period, where the switches T_1, T_4 or T_2, T_3 are on, is defined as follows:

$$t_1 - t_0 = t_3 - t_2 = T(1 - D) \tag{33}$$

Considering (28), (33), the rms values of the switch current, diode current and the input current can be calculated[see (34), (35) at the bottom of the page]:

$$I_{T1,RMS} = \sqrt{ \frac{1}{T} \left(\frac{4\left(\frac{I_{1,min}}{2} + \frac{(V_i\ddot{u} - V_o)(1-D)T}{2L_3\ddot{u}} + \frac{V_i(D-0,5)T}{2L_3} \right)^3 L_3 - 4\left(\frac{I_{1,min}}{2} + \frac{(V_i\ddot{u} - V_o)(1-D)T}{2L_3\ddot{u}} \right)^3 L_3}{3V_i} + \frac{L_3\ddot{u}\left(I_{1,min} + \frac{(V_i\ddot{u} - V_o)(1-D)T}{L_3\ddot{u}} \right)^3 - I_{1,min}{}^3 L_3\ddot{u}}{3(V_i\ddot{u} - V_o)} \right) } \tag{34}$$

$$I_{D1,RMS} = \sqrt{\frac{1}{T}\left[\frac{1}{3}\frac{\left(\left(\frac{V_i\ddot{u}-V_o}{L_3\ddot{u}^2}-\frac{V_o}{L_1\ddot{u}^2}\right)(1-D)T+I_{2,min}\right)^3}{\frac{V_i\ddot{u}-V_o}{L_3\ddot{u}^2}-\frac{V_o}{L_1\ddot{u}^2}}-\frac{1}{3}\frac{I_{2,min}^3}{\frac{V_i\ddot{u}-V_o}{L_3\ddot{u}^2}-\frac{V_o}{L_1\ddot{u}^2}}\right]} \qquad (35)$$

$$I_{D1,avg} = I_{2,min}(1-D)+\frac{1}{2}(1-D)^2 T\left(\frac{V_i}{L_3\ddot{u}}-\frac{L_1+L_3}{L_1 L_3\ddot{u}^2}V_o\right) \quad (36)$$

From the Fig. 6 it can be seen that the switch is turned off at the full blocking voltage. During time periods $t_1...t_2$ and $t_3...t_4$ all switches conduct, the energy is not transferred to the output. All secondary diodes don't conduct. The diodes D_1, D_3 and D_2,D_4 are connected serial to the output voltage. The blocking voltage of all diodes at turn off during time periods $t_1...t_2$ and $t_3...t_4$ can be hence calculated:

$$V_{D1,off} = V_o/2 \qquad (37)$$

D. Current-fed push-pull converter

The current-fed full-bridge converter was mathematically analysed in [8]. This converter provides a galvanic isolation an hence should be connected to the fuel cell as shown in the Fig. 1. The step-up conversion ratio can be, as shown in [8], calculated:

$$\frac{V_o}{V_i} = \frac{\ddot{u}}{\left(1-2t_{ov}/T\right)} \qquad (38)$$

The blocking voltages of the transistor and the secondary diodes can be, as shown in [7], calculated:

$$V_{T1} = 2V_o/\ddot{u} \qquad (39)$$

$$V_{D1,mqx} = V_o \qquad (40)$$

To reduce the blocking voltage of the transistor the maximum turns ratio of the transformer is needed. The solution of (38) for the turns ratio is:

$$\ddot{u}_{max} = V_o(1-D_{min})/V_{i,max} = 750V\cdot(1-0{,}5)/60V \approx 24 \quad (41)$$

The waveforms of this converter are identical with the current-fed full-bridge converter. The blocking voltage of the switch is twice as high as in full-bridge converter. The equations (34)-(36) are valid for the current-fed push-pull converter with $\ddot{u} = W_2/2W_1$.

E. Voltage-fed full bridge converter

The voltage-fed full bridge converter was mathematically analysed in [3]. This converter provides a galvanic isolation an hence should be connected to the fuel cell as shown in the Fig. 1. The minimum turns ratio of the transformer [3]:

$$\ddot{u}_{min} = \frac{V_o}{2V_{i,min}D_{max}} = \frac{750V}{2\cdot 30V\cdot 0{,}5} \approx 28 \qquad (42)$$

The maximum duty cycle cannot be increased above 50%. Decreasing of the duty cycle results in increasing of the turns ratio of the transformer and increasing of rms and maximum value of the switch current. The blocking voltages of the

transistor and the secondary diodes can be, as shown in [9], calculated:

$$V_{T1} = V_i \qquad (43)$$

$$V_{D1,max} = V_o \qquad (44)$$

It can be seen from (43) that the blocking voltage of the switch does not depend on duty cycle and turns ratio of the transformer. The conclusion of these thoughts is that the efficiency will be lower with the decreasing of maximum duty cycle. The duty cycle of 50% is practically unrealizable. Hence a little bit smaller duty cycle of 45% was determined. The simulation results for these parameters are shown in the Fig. 7.
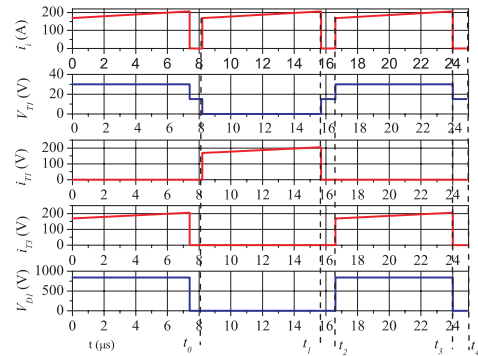

Fig. 7 Simulated waveforms of the voltage-fed full-bridge converter

During time periods $t_1...t_2$ and $t_3...t_4$ all switches are turned off, the energy is not transferred to the output. The switches T_1, T_4 and T_2,T_3 are connected serial to the input voltage. The blocking voltage of all switches during time periods $t_1...t_2$ and $t_3...t_4$ can be hence calculated:

$$V_{T1,off} = V_{T1,on} = \frac{V_i}{2} \qquad (45)$$

It was considered during the calculation of the switching loss that all switches are turned on and off at the half of the input voltage. The diodes are turned off at the voltage, which is equal to the output voltage. The time equations of the waveforms in [2] for the time periods $t_0...t_1$ and $t_2...t_3$ are the same as for the extended forward converter for the time period $t_0...t_1$. Considering (42), the rms, average values of the switch current, diode current and the input current can be calculated [see (47), (48)at the bottom of the page]:

$$I_{D1,avg} = I_{2,min}D + \frac{V_i\ddot{u}(1-2D)D^2 T}{2L_o} \qquad (46)$$

$$I_{T1,RMS} = \sqrt{\frac{1}{T}\left(\frac{1}{3}\frac{\left(V_i DT\left(L_o + L_1\ddot{u}^2 - 2L_1 D\ddot{u}^2\right) + I_{1,\min}L_1L_o\right)^3}{V_i L_1^2 L_o^2\left(L_o + L_1\ddot{u}^2 - 2L_1 D\ddot{u}^2\right)} - \frac{1}{3}\frac{I_{1,\min}^3 L_1 L_o}{V_i L_o + V_i L_1\ddot{u}^2(1-2D)}\right)} \qquad (47)$$

$$I_{i,RMS} = \sqrt{\frac{1}{T}\left(\frac{2}{3}\frac{\left(V_i DT\left(L_o + L_1\ddot{u}^2 - 2L_1 D\ddot{u}^2\right) + I_{1,\min}L_1L_o\right)^3}{V_i L_1^2 L_o^2\left(L_o + L_1\ddot{u}^2 - 2L_1 D\ddot{u}^2\right)} - \frac{2}{3}\frac{I_{1,\min}^3 L_1 L_o}{V_i L_o + V_i L_1\ddot{u}^2(1-2D)}\right)} \qquad (48)$$

$$I_{D1,RMS} = \sqrt{\frac{1}{T}\frac{\left(I_{2,\min}+\frac{V_i\ddot{u}(1-2D)DT}{L_o}\right)^3 L_o - I_{2,\min}^3 L_o}{3V_i\ddot{u}(1-2D)}} \qquad (49)$$

$$I_{i,avg} = 2I_{1,\min}D + \frac{V_i D^2 T\left(L_o + L_1\ddot{u}^2(1-2D)\right)}{L_1 L_o} \qquad (50)$$

E. Asymmetrical bridge double forward converter

The asymmetrical full bridge converter was mathematically analysed in [3]. This converter provides a galvanic isolation an hence should be connected to the fuel cell as shown in the Fig. 1. The maximum duty cycle can be determined at same way as for voltage-fed full-bridge converter. The minimum turns ratio of each transformer can be, as shown in [3], calculated:

$$\ddot{u}_{\min} = \frac{V_o}{2V_{i,\min}D_{\max}} = \frac{750V}{2\cdot30V\cdot0,5} \approx 28 \qquad (51)$$

The simulation results for these parameters are shown in the Fig. 8. The blocking voltages of the transistor and the secondary diodes can be, as shown in [2], calculated:

$$V_{T1} = V_i \qquad (52)$$

The transformer of the forward converter with a switch T_1 is magnetized during the time period $t_0...t_1$. The demagnetization of the transformer occurs during the time period $t_2...t_3$. During the time period $t_3...t_4$ the primary voltage of the transformer is null. Hence the switches T_1 and T_2 are connected serial to the input voltage. The switching off voltage of the switch T_1 is

$$V_{T1,off} = 0,5V_i \qquad (53)$$

During the time period $t_2...t_3$ the forward converter with a switch T_3 transfers the energy to the output. In this operational state the sum of secondary voltage of two transformers is a blocking voltage of diode D_5:

$$V_{D5} = 2V_i\ddot{u} \qquad (54)$$

During the time periods $t_1...t_2, t_3...t_4$ all two forward converters don't transfer the energy to the output. The secondary voltage of each transformer is a blocking voltage of diode D_1 and D_3. The voltage of the diodes at their turn off can be hence calculated:

$$V_{D1,off} = V_{D3,off} = 2V_i\ddot{u} \qquad (55)$$

The free-wheeling-Diode D_2 doesn't conduct during the time periods:

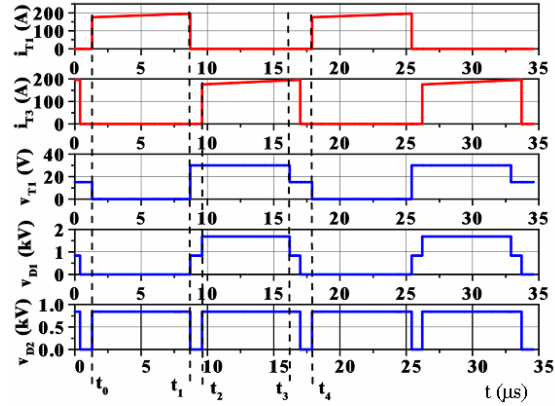$$t_1 - t_0 = t_3 - t_2 = DT \qquad (56)$$

Fig. 8 Simulated waveforms of the asymmetrical bridge double forward converter

The secondary voltage of the transformer is the blocking voltage of the free-wheeling diode. This voltage can be thus calculated:

$$V_{D2} = V_i\ddot{u} \qquad (57)$$

The free-wheeling diode is turned off at the full blocking voltage. The switches are, as in the case of full-bridge converter, turned on at the time, where no current flows. The switch on current is not equal null, but the current rises very slowly at the time, where the blocking voltage is null. The switching on loss can be then neglected.

IV. METHODS AND RESULTS OF COMPARISON OF DC/DC-CONVERTERS

A. Calculation of the efficiency

For the calculation of the efficiency the semiconductors for the switches and diodes of the circuits must be defined. This definition was done regarding to the calculated maximum voltage stress at the input voltage V_i=60V and maximum current stress at the input voltage V_i=30V. For the diodes of all circuits was the diode of type DSEP 9-06CR used. To simplify the calculation, MOSFET of the same type for the switches of all DC/DC-converter was chosen. The on-resistance of the MOSFET was for each circuit calculated recording to the formula [3]:

$$R_{DS,on} \sim V_{T,\max}^{2,6} \qquad (58)$$

The conduction losses of the switch can be calculated [3]:

$$P_{V,cond(T)} = R_{DS,on}\cdot\frac{I_{T,RMS}^2}{N_T} \qquad (59)$$

With $I_{T,RMS}$ – rms value of the switch current, N_T – number of parallel connected MOSFET for one switch.

The switching losses of the MOSFET could be calculated regarding to the measured switching losses, Fig. 9. The measured switching losses can be converted into the values for certain values of the over current and switching on and off voltages. To simplify the calculation, it was considered that 50% of the on switching loss is direct proportional to the over current and another 50%
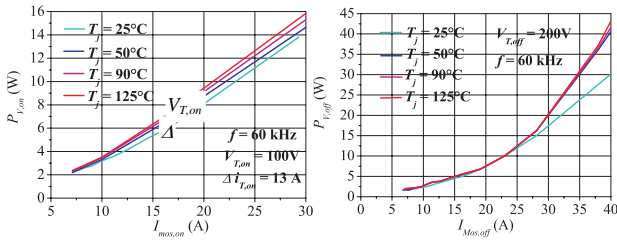

Fig. 9 Measured on and off switching losses at hard turn on and turn off as a function of on and off switching current for the MOSFET IXTH88N30P

is direct proportional to the switching on voltage. The switching off loss is direct proportional to the switching off voltage. The conduction loss of the diode can be calculated [3]:

$$P_{V,cond(D)} = r_d \cdot I_{D,RMS}^2 / N_D + V_{T0}I_{D,avg} \qquad (60)$$

With r_d – differential resistance, V_{T0} – threshold voltage, N_D – number of parallel connected diodes.

The switching loss of the diodes was calculated regarding to the approximated waveforms, which are shown in Fig. 10.
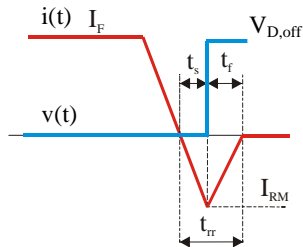

Fig. 10 Used for the calculation approximated waveforms of voltage and current of the diodes at turn off

The switching loss of the diode can be then calculated:

$$P_{REC} = 0.5 V_{D,off} I_{RM} t_f f \qquad (61)$$

With t_f – fall time of the reverse-recovery-current, I_{RM} – maximum value of reverse-recovery-current, f – switching frequency.

The maximum value of reverse-recovery-current can be taken from the datasheet. The rise time of reverse-recovery-current can be calculated:

$$t_s = \frac{I_{RM}}{di_F / dt} \qquad (62)$$

The fall time of reverse-recovery-current can be calculated:

$$t_f = t_{rr} - t_s \qquad (63)$$

After the calculation of all losses in the circuit the junction temperatures of all semiconductors must be calculated. It was considered that all semiconductors are placed on the same heat sink. The junction temperature of on the transistor T_1 and the diode D_1 can be calculated:

$$T_{j(T_1)} = T_a + P_{V(T_1)}\left(\frac{R_{th(jc),T_1}}{N_T} + \frac{R_{th(ck)}}{N_T} + R_{th(ka)}\right) + \sum_{k=1}^{n_D} P_{V(D_k)}R_{th(ka)} + \sum_{k=2}^{n_T} P_{V(T_k)}R_{th(ka)} \qquad (64)$$

$$T_{j(D_1)} = T_a + P_{V(D_1)}\left(\frac{R_{th(jc),D_1}}{N_D} + \frac{R_{th(ck)}}{N_D} + R_{th(ka)}\right) + \sum_{k=1}^{n_D} P_{V(T_k)}R_{th(ka)} + \sum_{k=2}^{n_T} P_{V(D_k)}R_{th(ka)} \qquad (65)$$

With $R_{th(jc),T_k}$ – junction to case thermal resistance of the MOSFET (can be taken from the datasheet), $R_{th(ck)} = 1,5 K/W$ – case to heat sink thermal resistance, $R_{th(ka)}$ – heat sink to ambient thermal resistance, n_D – total number of diodes in the circuit, n_T – total number of switches in the circuit, $P_{V(T_k)}$ – total loss for one switch, $P_{V(D_k)}$ – total loss for one diode, T_a – ambient temperature, N_T – number of parallel connected semiconductors for one switch, N_D – number of parallel connected semiconductors for one diode.

After calculation of the junction temperature the new parameter of the semiconductors for this temperature can be calculated. The loss for this parameter must be then calculated. The loss for the new parameter and the loss for the old parameter are compared. The iteration will continue until this difference has a minimum value. The goal of the calculation is to determine the number of transistors for each circuit that are needed to keep the junction temperature of the MOSFETs at the definite value $T_j = 92°C$. This value is identical for all circuits. Hence the expense for the semiconductors for each circuit can be seen. The results of the calculation are presents in the Table I.

B. Calculation of the expense for filter and for transformer

The minimum core-cross section of the transformer that is sufficient to provide that the transformer will not saturate can be regarding to [3] calculated:

$$A_{K,min} = \frac{V_{L1}DT + L_1 I_0}{N_1 \Delta B_{max}} \qquad (66)$$

With V_{L1} – primary voltage of the transformer, L_1 – magnetizing inductance, N_1 – number of turns at the primary side, I_0 – constant component in the magnetization of the transformer, ΔB_{max} – maximum magnetic flux swing.

The maximum magnetic flux swing was determined in consideration that the transformer will not saturate. For the circuits with the utilization of the B-H-characteristic of the transformer in all quadrants the magnetic flux can change from negative value to positive. The flux swing can be then double. The size of the transformer of DC/DC-converters is compared at the same utilization of the transformer for each circuit.

The length of magnetic path that corresponds to the calculated core-cross-section can be then determined with the

help of the datasheets of ferrite cores. The copper loss in the primary or secondary winding in the transformer [3]:

$$P_{V,CU1(2)} = \rho l_m N_{1(2)} I_{L1(L2),RMS}^2 / A_{CU1(2)} \qquad (67)$$

With l_m –length of magnetic path, $N_{1(2)}$ –number of turns of the primary or secondary winding, $A_{CU1(2)}$ –copper area for the primary or secondary winding, $I_{L1(L2),RMS}$ –rms value of current in the primary or secondary winding, $\rho = 1{,}724 \cdot 10^{-6}\,\Omega \cdot cm$ – resistance per unit length for copper.

The copper area for the primary or secondary winding can be calculated [3]:

$$A_{CU1(2)} = \frac{I_{L1(L2),RMS}}{j_{max}} \qquad (68)$$

With $j_{max} = 4\text{A/mm}^2$ – maximum current density in the winding.

The magnetization losses of the transformer $P_{V,fe1}$ at the defined magnetic induction B_1 and defined frequency f_1 can be determined from the datasheet of the core. The magnetization losses at the another magnetic induction B_2 and another frequency f_2 are [3]:

$$P_{fe2} = P_{V,fe1} \cdot (B_2 / B_1)^\gamma \cdot (f_2 / f_1)^\beta \qquad (69)$$

With $\gamma=1{,}45$, $\beta=2{,}7$ for ferrite materials [3].

The calculated losses are shown in the Fig. 10. The efficiency, calculated in the Table I, considers the total semiconductor loss and total transformer loss.

TABLE I
CALCULATED CURRENT AND VOLTAGE STRESSES, EFFICIENCY OF THE DC/DC-CONVERTERS
(T_j=92°C, $R_{th(KA)}$=0,1K/W, V_i=30V, V_o=750V, f=60kHz, V_o=750V, P_o=5kW, N_1=9, ΔB_{max}=0,3T; * – V_o=375V, P_o=2,5kW; **–ΔB_{max}=0,6T)

| Value — Nr. of circuit	$I_{T1,RMS}$ (A)	$I_{D1,RMS}$ $I_{D2,RMS}$ $I_{D3,RMS}$ (A)	$I_{D1,avg}$ $I_{D2,avg}$ $I_{D3,avg}$ (A)	$I_{i,RMS}$ (A)	$I_{i,avg}$ (A)	Δi_i (/)	$I_{D1,RM}$ $I_{D2,RM}$ $I_{D3,RM}$ (A)	$t_{rr(D1)}$ $t_{rr(D2)}$ $t_{rr(D3)}$ (ns)	$V_{D1,off}$ $V_{D2,off}$ $V_{D3,off}$ (V)	$V_{T1,on}$ $V_{T1,off}$ (V)	$\Delta i_{T,on}$ (A)	$V_{T1,max}$ (V_i=60V) (V)	$R_{DS(on)T1}$, (T_j=25°C) (mΩ)	$V_{D1,max}$ $V_{D2,max}$ $V_{D3,max}$ (V)	η (%)	Si-area for transistors (%)	$A_{K,min}$ (mm²)
1	94,3* (D=0,7)	12,3*	6,7*	95,5*	85,5*	0,5*	15*	37*	500*	100* 100*	75*	125*	27,5*	625*	90,6	276	308
2	109* (D=0,57)	5,4* 4,6* 10,5*	3,8* 3* 6,7*	109*	84,2*	0,8*	13* 12* 8,5*	34* 30* 42*	653* 540* 75*	73* 73*	8,5*	80*	8,5*	1080* 1171* 100*	94,3	100	166
3	98 (D=0,76)	6,5	3,2	166,7	166,7	0	15	37	375	62,5 62,5	90	62,5	5,3	750	90,3	366,7	100,5 **
4	102,2 (D=0,76)	6,8	3,3	166,7	166,7	0	15	37	375	125 125	90	125	27,5	750	91,3	300	201 **
5	143 (D=0,45)	5,2	3,8	182	172	0,35	12	31	750	15 15	336	60	4,3	750	93,6	138	41,6 **
6	141,1 (D=0,45)	4,5 2,1	3,5 0,6	182	172	0,35	12 12	31 31	840 1680	30 15	150	60	4,3	1680 1680	92,4	161	83,5
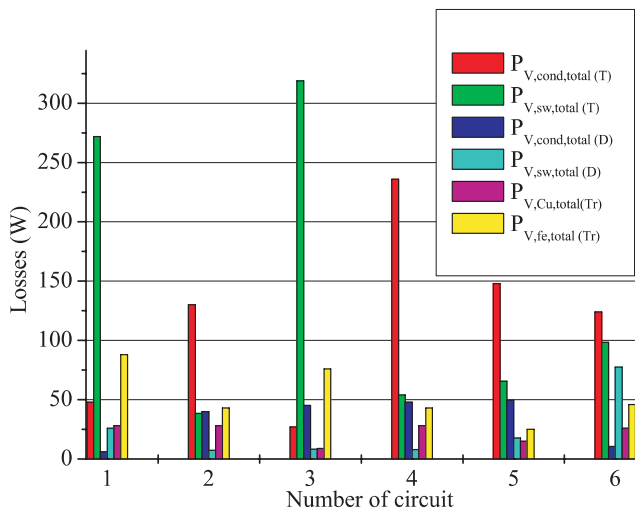
Fig. 11 Calculated losses of the DC/DC-converters

The relative input current ripple can due to [6] be defined as:

$$\Delta i_i = \sqrt{\frac{I_{i,RMS}^2}{I_{i,avg}^2} - 1} \qquad (70)$$

The higher current ripple causes the larger input filter. The calculated values for the current ripple are shown in the Table I. It can be seen that the current-fed circuits have minimum input current ripple. The extended forward converter has the highest current ripple because of not to high duty cycle. The criterion for the determination of the duty cycle was possible highest efficiency. The required core cross section of the transformer is minimum for the voltage-fed full-bridge converter. The DC/DC-converter with a quite high duty cycle (boost converter with tapped inductor, extended forward converter) requires a larger transformer.

V. CONCLUSIONS

Six circuits of the DC/DC-converter for the input voltage V_i=30V, output voltage V_i=750V, the output power P_o=5 kW and the switching frequency f=60kHz were mathematically analyzed. The results of the analysis are the rms, average values of the switch and diode currents, the maximum voltage

stresses of the switches and diodes, the switch and diode voltages at turn on and turn off. These values were used for the calculation of the efficiency, relative input current ripple and the minimum size of the transformer. The extended forward converter has the highest efficiency of 94,3% and the boost converter with tapped inductor has the lowest efficiency of 90,3%. For the extended forward converter the lowest number of transistors is needed.

REFERENCES

[1] E. Santi, D. Franzoni, D. Monti, A. Patterson, F. Ponsi, F. Barry "A fuel cell based uninterruptable power supply" *IEEE Applied Power Electronics Specialist Conference*, 2002, Proceedings on CD-ROM
[2] O. Krykunov, „*Analysis of the Extended Forward Converter for Fuel Cell Applications"*, ISIE, 2007
[3] Robert W. Erickson, *Fundamentals of Power Electro* (Book style)*, University of Colorado*, 1997
[4] T. A. Nergaard, J. F. Ferrell, L. G. Leslie, and J. S. Lai, "*Design considerations for a 48V fuel cell to split single phase inverter system with ultra capacitor energy storage"*, *IEEE Applied Power Electronics Specialist Conference*, 2002
[5] T. Meyer, "DC/DC-Wandler mit kleiner Eingangsspannung für photovoltaische, elektrochemische und thermoelektrische Zellen", Fortschr.-Ber. VDI, R. 21, Nr. 288, Düsseldorf, VDI-Verlag, 2000
[6] H. Solmecke, "*Optimierter Stromrichter für Brennstoffzellenanlagen*" Dissertation, Hagen, 1998
[7] I. Merfert, O. Krykunov, A. Lindemann, "*High-power tapped-inductor boost conevrter fot Fuel Cell Applications*", PCIM, 2005
[8] Tarter, E. Ralph, „Solid-state power conversion handbook*"*, 1993